

Morphological study of cationic polymer–anionic surfactant complex precipitated in solution during the dilution process

M. MIYAKE and Y. KAKIZAWA, *Functional Materials Research Laboratories (M.M.) and Beauty Care Research Center (Y.K.), Lion Corporation, 2-1 Hirai 7-Chome, Edogawa-ku, Tokyo 132-0035, Japan.*

Accepted for publication March 16, 2010.

Synopsis

We investigated the phase diagrams and the morphology of the complexes that were formed by cationic polymers, cationic cellulose (CC) and cationic dextran (CD), and by anionic surfactant-based sodium poly(oxyethylene) lauryl ether sulfate (LES). The anionic charge of the LES-based surfactants was changed by adding an amphoteric surfactant, lauryl amidopropyl betaine acetate (LPB), or a nonionic surfactant, polyoxyethylene stearyl ether (C₁₈EO₂₅). We discuss the relationship between the complex aggregation process and the morphology of the precipitated complexes. The morphologies of CC complex aggregates, which precipitated during the dilution process in a model shampoo solution, changed from membranous forms to mesh-like forms by decreasing the charges of both the CC and the surfactant. Their touch on hair in the rinsing process changed from sticky to smooth and velvety, corresponding to their rheological properties. In contrast, CD complex aggregates had a membranous form and a smooth touch independently of the charges on the polymer and surfactant. These results suggested that the control of the charges of both the polymer and surfactant and the choice of polymer structure are important for excellent conditioning effects upon rinsing with shampoo.

INTRODUCTION

Polymers and surfactants are important materials in the fields of cosmetics and toiletries. The variety of properties generated from the interaction of these materials determines the functions of the final products. In particular, the so-called trigger system, in which dilution of the solution causes complexes formed between oppositely charged polymers and surfactants to precipitate, is the basic mechanism in conditioning shampoos these days (1). Since anionic surfactants are the basic material in cleaning agents, cationic polymers represented by cationic cellulose are utilized in shampoo (2–5). The complexes coacervated through dilution adhere to hair, prevent hair entanglement in the rinsing process, and promote the adhesion to hair of emollients such as silicone, thereby producing a conditioning effect (6,7). The efficiency of shampoo is controlled by varying polymer species and by surfactant composition, and these factors determine the touch of hair in rinsing (8,9).

Address all correspondence to M. Miyake.

Complex precipitation (CP) regions have been systematically studied in terms of phase diagrams in basic research on the interaction between oppositely charged polyelectrolytes and surfactants (10–12). The binding of surfactants to polymers was the main subject of these studies at surfactant concentrations lower than those used in the precipitation region (13–15), and the structure of solubilized complexes in solution was also observed (16). In contrast, the complexes were solubilized due to the adsorption of surfactant micelles at higher surfactant concentrations in the CP region. The interactions between polymer chains and micelles increased with the increasing anionic charge of the surfactant (17) and with the decreasing concentration of the surfactant (18), and the shielding effect of salts was also revealed to affect the interaction (19,20). The solubilized complexes near the CP region were observed to grow in size probably because of the decreasing surfactant and salt concentrations in the solution (18).

Shampoos contain anionic surfactants at high concentrations where cationic polymers are solubilized in micelles; however, the change in the CP region by mixing amphoteric and nonionic surfactants and the morphology of the surfactant–polymer complexes deposited during the dilution process of the shampoo solution have not been investigated systematically.

The present study aims to develop the relationship between the mixed surfactant composition and the complex precipitation during the dilution process and to observe the morphology of the complexes precipitated by the dilution of a model shampoo solution, which contains typical cationic polymers used in shampoo, cationic cellulose and cationic dextran, and anionic surfactants with LES as the base component. In addition, the relation between the morphology and rheological properties of complex aggregates on the hair surface was elucidated, and the effects of the structure of the polymer molecules and the composition of the surfactants on the morphology are discussed.

MATERIALS AND METHODS

MATERIALS

Three kinds of cationic cellulose (CC) were obtained from Lion Chemical Co. (Leogarde[®] series). The degrees of cationic substitution per unit of glucose (α) were 0.38, 0.21, and 0.10, and the average molecular weights determined by light scattering were 5.3×10^5 , 5.1×10^5 , and 5.5×10^5 , respectively. Cationic dextran (CD) was obtained by the reaction of dextran (Meito Sangyo Co., Ltd.), with a molecular weight of about 2×10^5 , with glycidyltrimethylammonium salt in solution in the presence of NaOH as a catalyst in a nitrogen stream, and the product was neutralized and dried. The values of the degrees of cationic substitution of the obtained CD were 0.30 and 0.38. Figure 1 shows their chemical structures.

Anionic sodium poly(oxyethylene) lauryl ether sulfate (LES, with a mean oxyethylene chain length of 3 mol), and amphoteric lauryl amidopropyl betaine acetate (LPB) were purchased from Taiko Oil & Fat Company and Ipposha Oil Industries Co., Ltd, respectively. Nonionic poly(oxyethylene) stearyl ether (C₁₈EO₂₅) was supplied by Nihon Emulsion Co., Ltd. All of these surfactants were used as supplied. The salt used to adjust the ionic strength of the solution was reagent grade sodium sulfate (Na₂SO₄) (Tokyo Kasei Ind. Co.). All experiments were performed with distilled water.

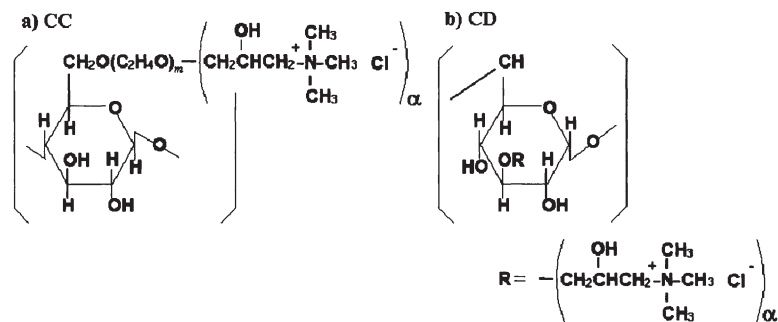


Figure 1. Chemical structures of cationic cellulose (CC) and cationic dextran (CD). $m = 2\text{--}3$. α is the degree of cationic substitution.

METHODS

Preparations of the phase diagrams and the model shampoo. The following method was performed to make solutions for phase diagram preparation. Given amounts of CC, surfactant, sodium sulfate, and water were weighed into a test tube with a screw cap, and the contents were well mixed at 60°C and equilibrated for several days. Afterward, the sample solution was visually checked to see whether there were any complex precipitates or not. The model shampoo solution for complex precipitation was prepared with a composition of 1wt% CC, 15wt% surfactant, and 3wt% electrolyte.

Observations of the morphology of the precipitated complex. The model shampoo solution was diluted ten times with water, and the complexes were allowed to deposit on a glass slide. The glass slide with the coacervate was immersed in 50 ml of acetone for one day. After this procedure was repeated three times, the coacervate on the glass slide was dried in a critical point drying apparatus, Model HCP-2 (Hitachi), using CO_2 , and the morphology of the dried sample was observed with an FE-SEM Model JSM-6300F (JOEL). The SEM images of the dried sample show the aggregated polymer chains because excess surfactants were removed by the acetone treatment.

Light-scattering measurements on the solubilized complex. The relative scattered light intensity I ($I = I_{90}(\text{sample})/I_{90}(\text{benzene})$) was measured on the polymer–surfactant complex dissolved in the model shampoo and diluted shampoo solutions by means of a light-scattering photometer, Model DLS-700 (Photal Co.), using an Ar laser at 75 mW. The relative scattered light intensities of the complexes were calculated using the following equation, according to an earlier paper (19):

$$\Delta I_{\text{complex}} = I_{\text{whole}} - I'_{\text{micelle}} \quad (1)$$

where I_{whole} is the relative scattered light intensity for the sample solution containing the polymer, surfactant, and salt. I'_{micelle} is the intensity for the solution containing no polymer but the same concentrations of surfactant and salt (Figure 2). Then, the $\Delta I_{\text{complex}}$ gives the scattered light intensity due to the polymer chains in the solubilized complexes, and it increases when the chains in the complex aggregate intra- and intermolecularly.

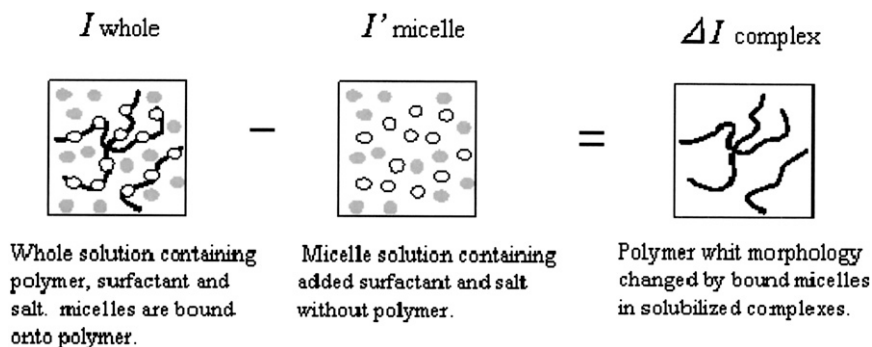


Figure 2. Relative scattered light intensity of solubilized complexes.

Evaluation of rheological properties. Rheological measurements on the precipitated complexes were conducted using an oscillatory rheometer, Model RS-100 (Haake Co.), with a corn-plate (diameter=20 mm, angle=1°) within an angular frequency range of $\omega = 0.05\text{--}650$ rad/sec. The Maxwell model for gels and polymer liquids (21–23) was used to calculate the parameters, i.e., the storage modulus of elasticity, G' , the loss modulus of elasticity, G'' , and the complex viscosity, η^* .

RESULTS AND DISCUSSION

DILUTION OF THE MODEL SHAMPOO SOLUTION AND COACERVATION OF THE COMPLEX

Figure 3a–c shows the partial phase diagrams for the systems consisting of CC ($\alpha = 0.38, 0.21, \text{ and } 0.10$), LES, salt, and water. The upper diagrams are for the systems containing 1wt% CC, and the lower ones are for those containing 0.1wt% CC. The filled circle in each of the upper diagrams represents the composition of the model shampoo solution (CC = 1wt%, LES = 15wt%, and $\text{Na}_2\text{SO}_4 = 3\text{wt } \%$) before dilution, and that in each of the lower diagrams gives the composition of the ten-times-diluted model shampoo solution. The compositions for the diluted solution were in the complex precipitation region (CP) when the values of α for CC were 0.38 and 0.21, whereas the composition for the diluted solution at $\alpha = 0.10$ lay in the region of a uniformly transparent solution (1Φ), though the CP region also appeared at lower concentrations of the surfactant and salt. During the dilution of the model shampoo solution, the complexes deposited in the solutions containing CC with $\alpha = 0.38$ and 0.21, while no precipitate was observed in the solution with $\alpha = 0.10$. Hence, proper choices for the polymer structure and solution composition are necessary to reach the diluted composition in the CP region.

PHASE DIAGRAMS BY MIXING SURFACTANTS AND THE MORPHOLOGY OF THE PRECIPITATED COMPLEX

Partial phase diagrams. Figure 4a–f shows the partial phase diagrams for CC with α values of 0.38 and 0.21. The anionic charge was varied by mixing LEB (Figure 4a–f) and $\text{C}_{18}\text{EO}_{25}$

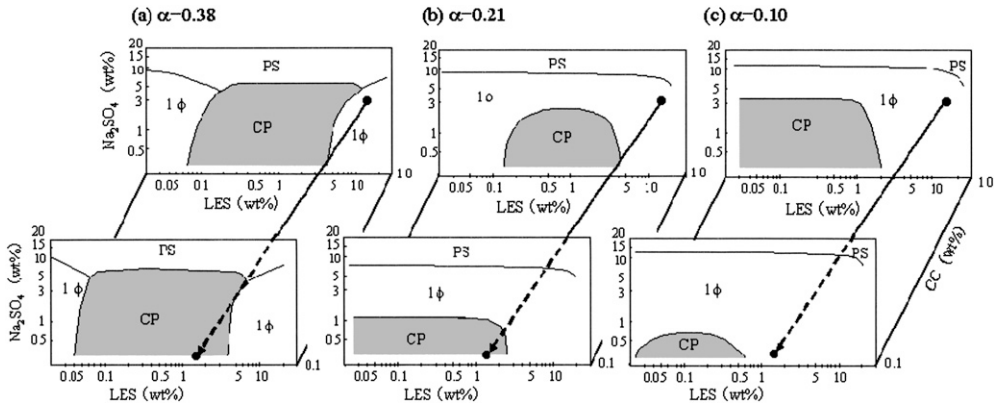


Figure 3. Partial phase diagrams in the presence of CC, LES, and Na_2SO_4 . In (a), (b), and (c), the degrees of cationization for CC are $\alpha=0.38$, $\alpha=0.21$, and $\alpha=0.10$, respectively. The arrows in these figures show the dilution process of the sample solution containing 1wt% CC, 15wt% LES, and 3wt% Na_2SO_4 . (CP = complex precipitation region, PS = phase separation region, and 1ϕ = clear one-phase solution.)

(Figure 5a–f) with LES. The CP region appeared in a wide zone of the phase diagram for the mixture of LES and CC at $\alpha = 0.38$ (Figure 4a and Figure 5a show the same data). This zone was connected to the phase separation (PS) region where salting out occurred to produce phase separation on the high salt concentration side. In contrast, the reduction in the α value shifted the CP region toward the lower concentration side of salt and

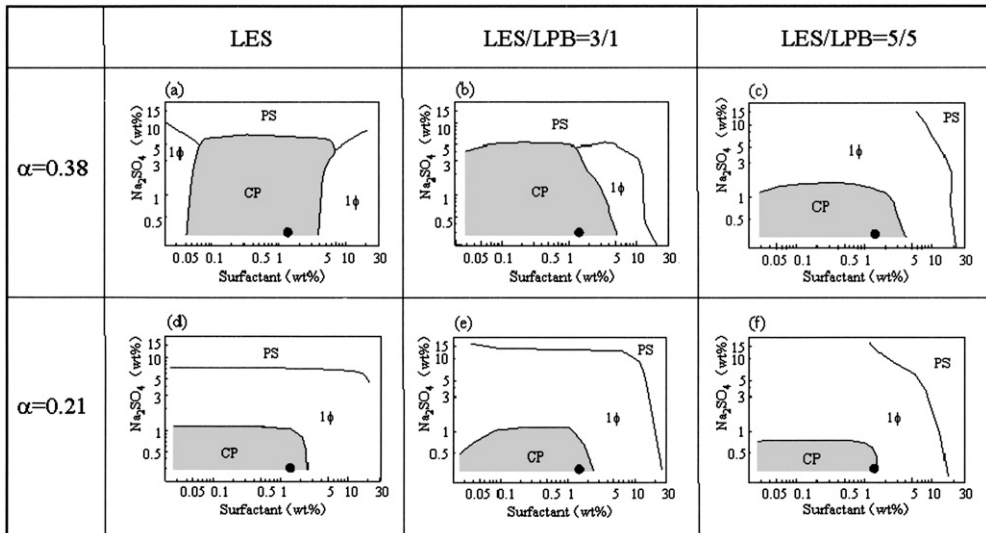


Figure 4. Effect of LPB mixing on the partial phase diagrams for systems containing CC at 0.1 wt%, surfactant, and Na_2SO_4 as salt. (a), (b), and (c) are for CC at $\alpha = 0.38$; (d), (e), and (f) are for CC at $\alpha = 0.21$. The mixing ratio of the surfactant is given by weight. (CP = complex precipitation region, PS = phase separation region, and 1ϕ = clear one-phase solution region.)

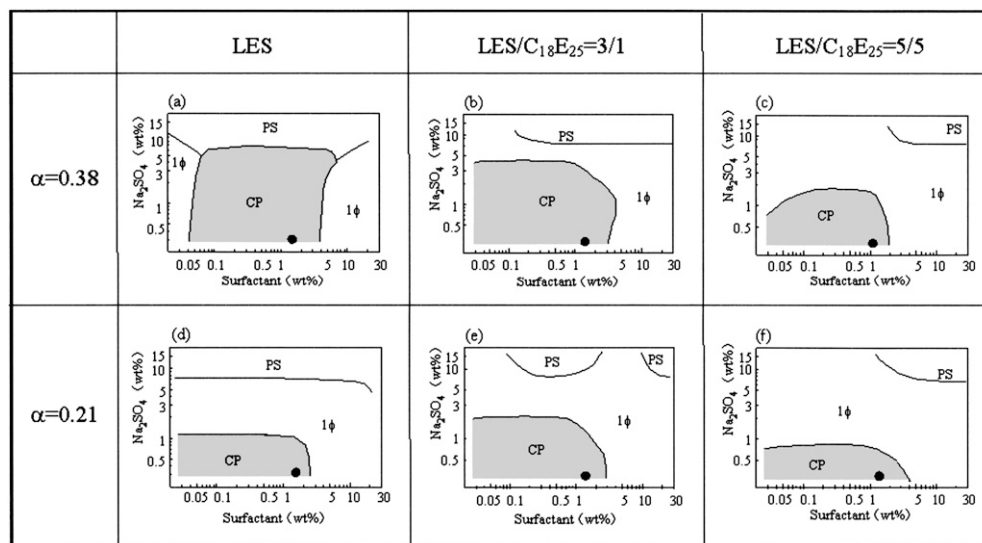


Figure 5. Effect of $C_{18}E_{25}$ mixing on the partial phase diagrams for systems containing CC at 0.1 wt%, surfactant, and Na_2SO_4 as salt. (a), (b), and (c) are for CC at $\alpha = 0.38$; (d), (e), and (f), are for CC at $\alpha = 0.21$. The mixing ratio of the surfactant is shown by weight. (CP = complex precipitation region, PS = phase separation region, and 1ϕ = clear one-phase solution region.)

surfactant, and caused the 1ϕ region to appear between the CP and PS regions. While the anionic charge of the micelles was lowered by mixing LPB and $C_{18}EO_{25}$ and the 1ϕ region widened (Figure 4b,c and Figure 5b,c, respectively), the CP region shifted to a small extent on the concentration axis of the surfactant. $C_{18}EO_{25}$ mixing with CC at $\alpha = 0.21$ tended to widen the CP region slightly (Figure 5e,f). Dilution produced complex precipitation for CC at $\alpha = 0.38$ and 0.21, even though the CP region shifted, because the composition of the diluted model shampoo (filled circle) still lay in the region. In contrast, the composition of the diluted shampoo solution was in the 1ϕ region for CC at $\alpha = 0.1$, even though the solution contained LPB or $C_{18}EO_{25}$, and no complex precipitation was observed, as shown in Figure 3c.

SEM images of the precipitated complexes. Typical SEM images of the complexes precipitated from the ten-times-diluted model shampoo solution are shown in Figure 6a–f for the system containing CC, LES, and LPB, and in Figure 7a–f for that containing CC, LES, and $C_{18}EO_{25}$. The complex precipitated from the system containing no LPB had a uniformly dense membranous morphology when α was 0.38 (Figure 6a and Figure 7a show the same data). In contrast, the addition of LPB produced an increase in the hollow parts in the SEM images (Figure 6b,c), while $C_{18}EO_{25}$ produced a network structure (Figure 7b,c). The system containing CC at $\alpha = 0.21$ and LES alone caused the complex to form a mesh-like structure (Figure 6d). The mesh size widened (Figures 6e and 7e), and eventually the complex precipitated in a dispersed state (Figures 6f and 7f), with an increase in the mixing ratio of LPB and $C_{18}EO_{25}$. Thus, the lowering of the degree of the polymer cationic charge and the anionic charge in the mixed micelles made the structure of the precipitated complex looser. Further charge reductions of both the polymer and the surfactant micelles prevented secondary complex aggregation.

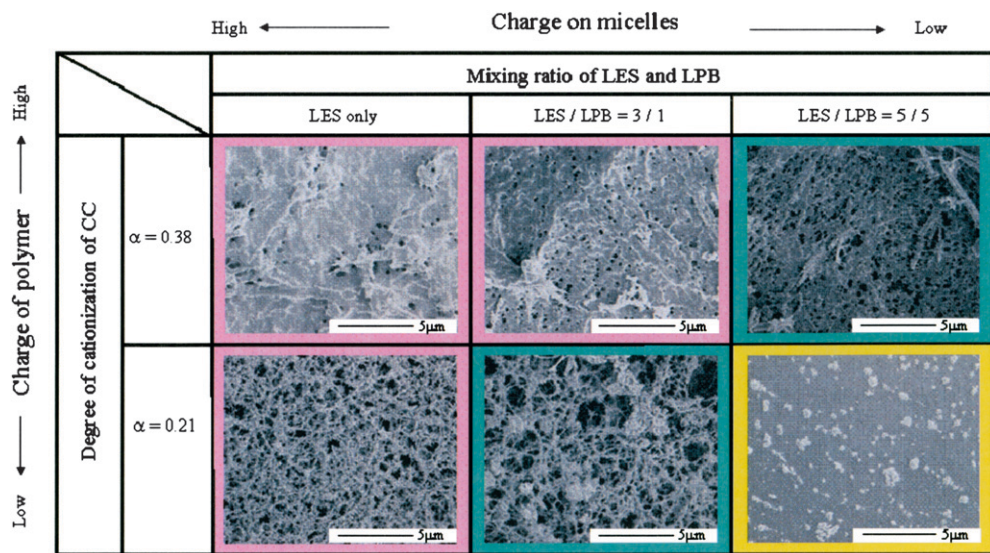


Figure 6. Effect of LPB mixing on the morphology of precipitated complexes from ten-times-diluted model shampoo solution.

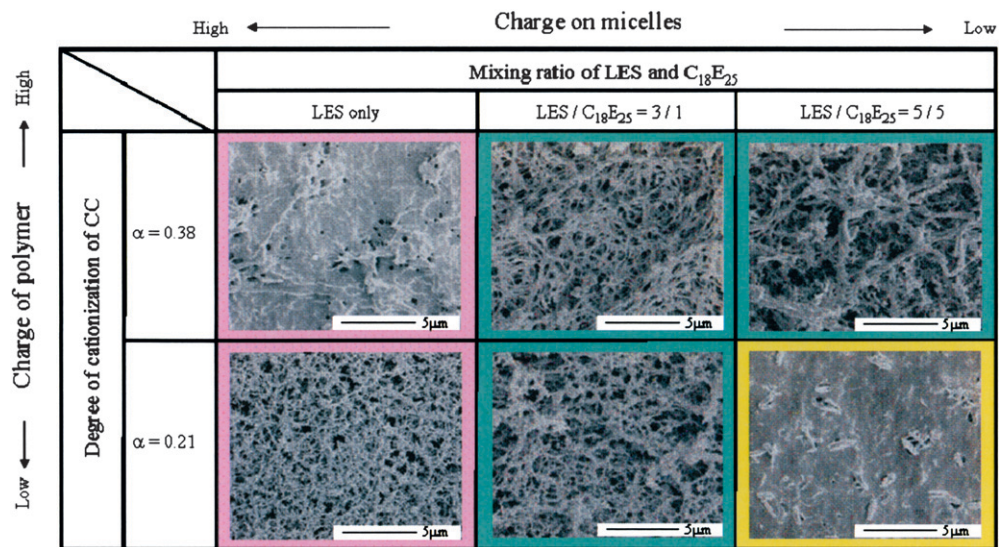


Figure 7. Effect of C₁₈E₂₅ mixing on the morphology of precipitated complexes from ten-times-diluted model shampoo solution.

STRUCTURE OF THE POLYMER CHAIN AND THE MORPHOLOGY OF THE PRECIPITATED COMPLEX

The relationship between the structure of the polymer chains and the morphology of the precipitated complexes was investigated. When compared with CC molecules in which

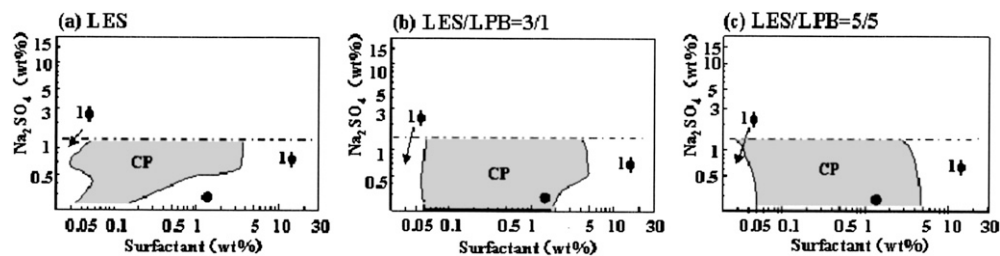


Figure 8. Partial phase diagrams for systems containing 0.1 wt% CD at $\alpha=0.38$, LES and LPB as surfactants, and Na_2SO_4 as salt at varied concentrations. The region above the dotted line was not observed.

glucose units are connected by β -1,4 bonds, CD molecules in which glucose units are connected through α -1,6 bonds have a higher bendability. Figure 8 shows the partial phase diagrams of the systems containing CD at $\alpha = 0.38$ and LES/LPB. The CP region for the system containing LES alone lay on the low surfactant concentration side of the diagram (Figure 11a), and it widened on the low salt concentration side when LPB was added to the system, bringing the composition of the diluted model shampoo solution into the CP region. The same trend was observed for the system containing less cationized CD at $\alpha = 0.30$. A comparison of the phase diagrams in Figure 8 with those for the systems containing CC at $\alpha=0.38$ (Figure 4a–c) revealed that no complex precipitation occurred in the dilution of the systems containing CD when the charge on the surfactant micelles was high. LPB mixing with CD at $\alpha = 0.38$ tended to widen the CP region on the lower salt concentration side, and the complexes coacervated in dilution (Figure 8b,c).

Figure 9a,b shows typical SEM images of complexes precipitated in the dilution process of the model shampoo solutions containing LES/LPB=3/1 and CD at $\alpha=0.38$, 0.30. Membranous aggregates of the complexes precipitated in both cases independently of the charge on CD.

MECHANISM OF THE MORPHOLOGY FORMATION OF THE COMPLEX AGGREGATES

The morphology of the complexes precipitated in the model shampoo solution changed according to the degree of cationic charge, the structure of the polymer chains, and the composition of the surfactant mixtures. The dilution of the model shampoo solution is likely to cause changes in the dissolved state of the complexes before the composition reaches the CP region. Figure 10 shows the changes in the relative scattered light intensity,

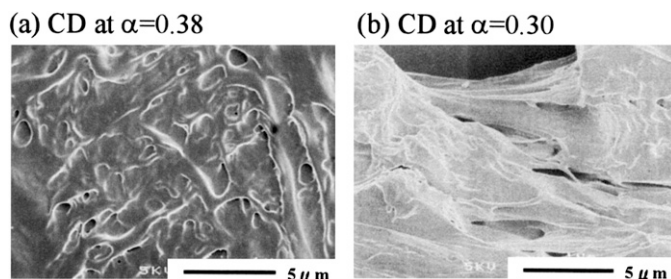


Figure 9. Effect of CD bendability on the morphology of the precipitated complex from ten-times-diluted model shampoo. Surfactant: LES/LPB=3/1.

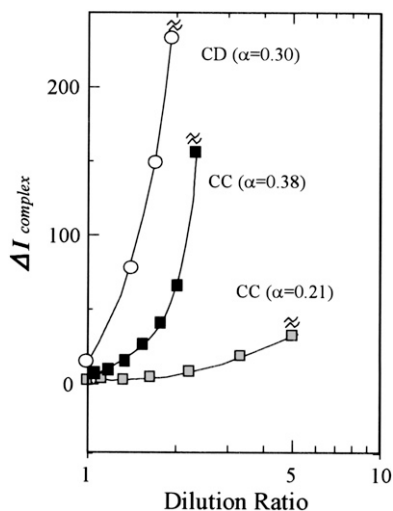


Figure 10. Change in relative scattered light intensity of the solubilized complex with increasing dilution ratio. Surfactant: LES/LPB=3/1.

$I_{complex}$, measured at varying compositions during dilution for the model shampoo solutions containing LES/LPB = 3/1 as a surfactant, CC with $\alpha = 0.38$ and 0.21, and CD with $\alpha = 0.30$ as the polymer. All model shampoo solutions were of 1ϕ until their compositions reached the highest dilution ratios in the figure. Their dilution produced increases in the relative intensity of the light scattered by the polymer-surfactant complex, and the formation of complex coacervates was observed when the solution composition was beyond those at the highest dilution ratios. The increase in the relative scattered light intensity, $I_{complex}$, means that the solubilized complexes adhered due to dilution. The $I_{complex}$ for CC before coacervation sharply increased when the cationic charge was high. The increase in the $I_{complex}$ was more abrupt for CD at $\alpha = 0.30$ than for CC at $\alpha = 0.38$. Table I shows the shape and size of the polymer in salt solution by SLS measurement. In fact, the shape of CC, with a rigid chain, was rod-like, and that of CD, with a bendable chain, was contracted and coil-like. In other words, CC and CD favorably assume a rod-like shape and a contracted coil-like shape in the model shampoo solution, respectively. As shown in Figure 11, in the complex adhesion by dilution, it is suggested that the coil-like complexes for CD densely gathered each other and that the rod-like complexes for CC cross-linked and essentially formed a mesh-like structure. The density of the contracted coil-like chain for CD caused a higher $I_{complex}$ than that of CC as well as an abrupt increase in the $I_{complex}$, even if the cationic charge and surfactant composition were the same. On the other hand, decreasing the $I_{complex}$ in CC complexes caused the mesh-like structure of the complexes precipitated to form. CC became looser. That means that the

Table I
Shape and Radius of CC and CD in 3wt% Na₂SO₄ Solution

	α	Shape	Radius (nm)
CC	0.38	Rod	116
	0.21	Rod	122
CD	0.30	Coil	36

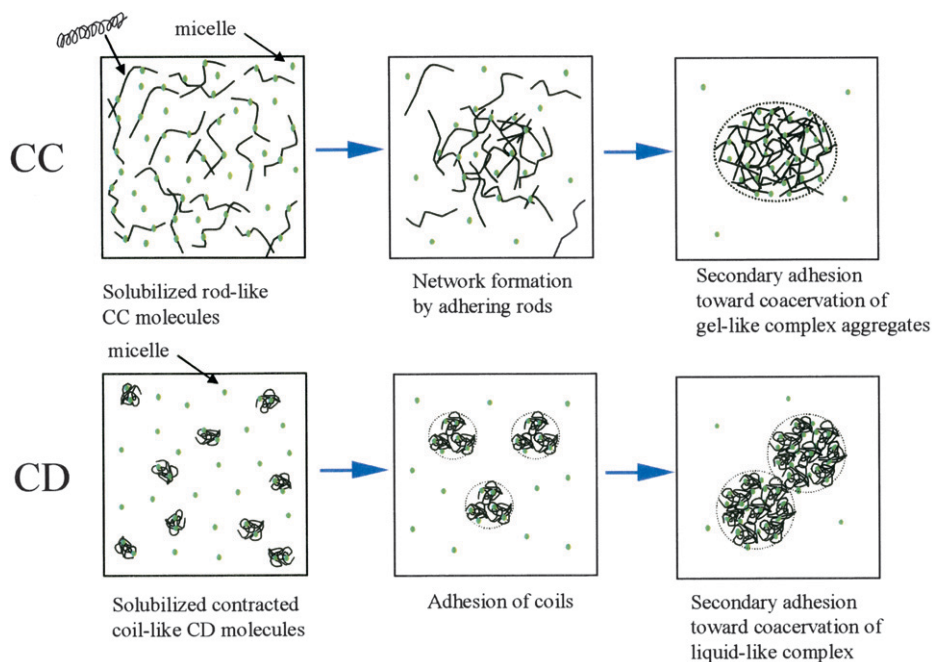


Figure 11. Difference between CC and CD in the coacervation process of cationic polymer and of anionic micelles in the dilution process.

cross-links of the rod-like complexes before coacervation were reduced by lowering the cationic charge. From these considerations, we found that the morphologies of the precipitated complexes were formed by the adhesion state of the solubilized complexes before coacervation, where the membranous structure was generated from the dense complex aggregates and the mesh-like structure from the looser complex aggregates.

RHEOLOGICAL PROPERTIES OF THE PRECIPITATED COMPLEXES AND THE TOUCH OF HAIR IN THE RINSING PROCESS

Polymer–surfactant complexes precipitated during dilution adhere to hair and determine its texture upon rinsing. Figure 12 shows the viscoelastic parameters for the complex consisting of CC at $\alpha = 0.38$ and LES, which leads to a membranous morphology, and that consisting of CC at $\alpha = 0.21$ and LES/LPB=3/1, which forms mesh-like aggregates. The former figure suggests the presence of a gel-like bridging structure in the precipitated complex because the curves for the storage modulus of elasticity, G' , and the loss modulus of elasticity, G'' , crossed at around $\omega = 10$ [rad/s] and the complex viscosity, η^* , decreased on the high frequency side. In contrast, the latter figure shows that η^* was low and independent of the frequency and that G' and G'' increased linearly, showing the fluid-like character of the complex. It is clear that the decrease in the cross-links of the rod-like CC complex is full of fluidity in the precipitated complexes. Figure 13 schematically shows the touch of the hair in the process of rinsing for the model shampoo solution. The precipitated complex consisting of CC at $\alpha = 0.38$ and LES, which formed dense membranous aggregates, gave a sticky touch, whereas the complex consisting of CC at $\alpha = 0.21$ and LES/LPB=3/1, which

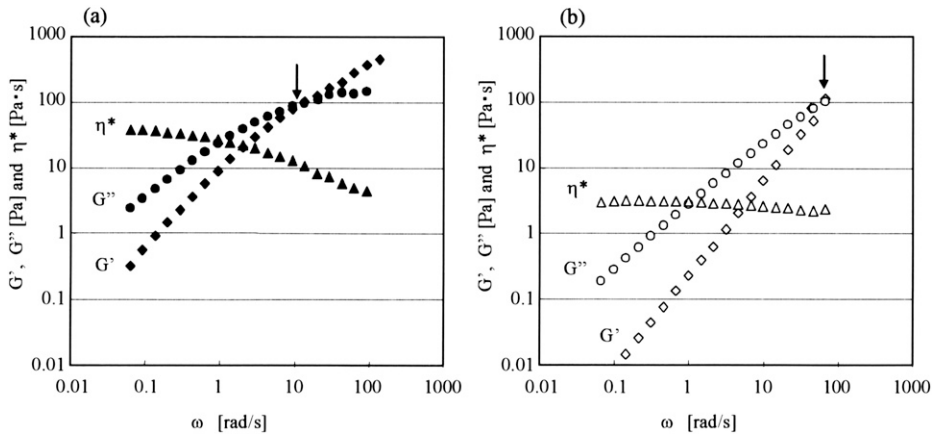


Figure 12. Rheological parameters, G' , G'' , and η^* , of precipitated complexes from ten-times-diluted solutions. (a) Model shampoo containing CC at $\alpha=0.38$ and LES; (b) model shampoo containing CC at $\alpha=0.21$ and LES/LPB=3/1.

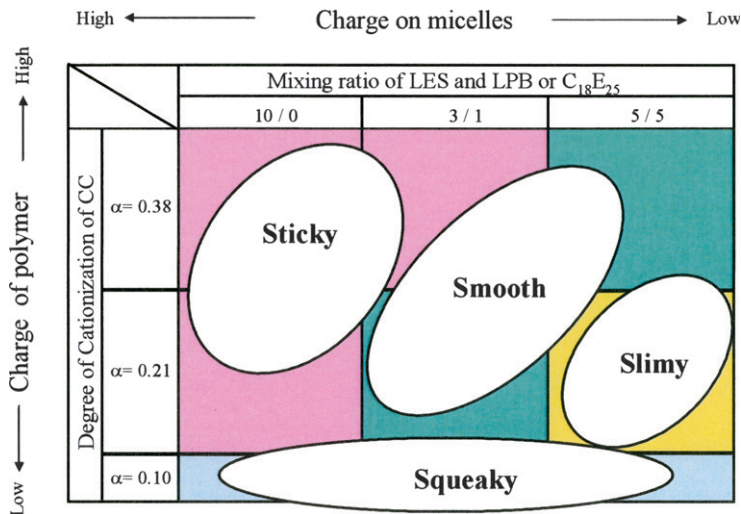


Figure 13. Touch of hair in the rinsing process of model shampoo solution.

formed mesh-like aggregates, showed a smooth touch. This suggested the large contribution of the rheological properties of the precipitated complexes to the touch upon rinsing. Moreover, the complex with lower charges in a dispersed state (CC at $\alpha = 0.21$ and LES/LPB=5/5) gave a somewhat oily touch. Surfactants adhering to hair with the complexes caused an oily touch because the rheological properties of the complexes were lower. In contrast, the touch upon rinsing was smooth for CD at $\alpha = 0.38$ and LES/LPB=3/1 (Figure 4a), even though the membranous morphology was close to that of CC at $\alpha=0.38$ and LES (Figure 6a). The rheological properties of the precipitated complexes for CD at $\alpha = 0.38$ and LES/LPB=3/1 were similar to those in Figure 12b (the data are not shown here). This suggests that the differences in the flexibility of the polymer chains in coil-like

complexes determine the rheological properties and the touch upon rinsing, even though the morphologies of the precipitated complexes are the same.

Practically, the touch in the rinsing process corresponds to the wet feel after shampooing. Other conditioning agents in shampoos, like silicon, and in conditioners have greater effects on the feel after drying. The membranous morphology in the complexes of CC led to a stiff feel after drying when much of the complex adhered to the hair. To realize a good dry feel, the control of morphology in the complexes and the adjustment of synergism between the precipitated complexes and other conditioning agents would be important.

CONCLUSIONS

The CP region in the phase diagrams that contained cationic cellulose (CC) or dextran (CD) and added anionic surfactant and the relative scattered intensity of solubilized complexes have been observed. The relationship between the morphology of the complexes precipitated by dilution of the model shampoo solution and the touch on hair has been studied, and the effects of the charges of the polymer and added surfactant and the structure of the polymer chain have been discussed.

CC molecules with rigid chains are favorable for rod-like complex conformation. It is considered that the rod-like complexes cross-linked and coacervated in the dilution process of the model shampoo solution. The complex aggregates precipitated from the model shampoo solution had a membranous morphology if both the CC and surfactant were highly charged; a mesh-like structure with openings was created and the aggregates were loosened when both charges were reduced. This suggested that the cross-links in the complex aggregates were reduced with decreasing charge and showed no precipitation if the charge of the polymer was low (for instance, if $\alpha = 0.1$).

In contrast, CD molecules with flexible chains are favorable for contracted coil-like complexes. No complex precipitated when the anionic charge on the surfactant was high, and the complexes precipitated if the anionic charge of the surfactant was reduced. CD led to membranous complex aggregates in the model shampoo solution even when the charges of the polymer and surfactant were lower. This suggested that the rod-like CC molecules and contracted coil-like CD molecules form different morphologies of complex aggregates, depending on the charge and structure of the polymer chains.

The touch of hair in the rinsing of the model shampoo with CC reflected the rheological properties that corresponded to the morphology of the precipitated complexes. The CC complex aggregates gave a smooth touch when they showed a loose mesh-like morphology. In contrast, CD complex aggregates gave a smooth touch even though they exhibited a membranous morphology, probably because of the flexibility of the CD polymer. These results suggested that the control of the charges of both the polymer and surfactant and of the choice of the polymer structure is important for excellent effects in the rinsing of shampoo. Moreover, silicone and other oils are mixed in shampoos nowadays. Thus, the complex aggregates involve these agents when they precipitate from the shampoo solution. The morphology of complex aggregates in this work would closely relate to the deposition of silicone. The control on the morphology of complex aggregates is important for excellent conditioning effects.

ACKNOWLEDGMENTS

The authors express their sincere appreciation to Dr K. Sugiyama, Director Executive General Manager of Research & Development Headquarters, Lion Co., and N. Yamamoto, Director of Functional Materials Research Laboratories, Lion Co.

REFERENCES

- (1) E. D. Goddard, "Polymer/Surfactant Interaction in Applied Systems," in *Cosmetic Science and Technology Series, Vol. 22. Principles of Polymer Science and Technology in Cosmetics and Personal Care* (New York, Marcel Dekker, 1999), pp. 181.
- (2) B. Idson, "Polymers as Conditioning Agents for Hair and Skin," in *Cosmetic Science and Technology Series, Vol. 21. Conditioning Agents for Hair and Skin* (New York, Marcel Dekker, 1999), pp. 251.
- (3) E. D. Goddard, T. S. Phillips, and R. B. Hannan, Water soluble polymer-surfactant interaction—Part I, *J. Soc. Cosmet. Chem.*, **26**, 461–475 (1975).
- (4) E. D. Goddard and R. B. Hannan, Polymer/surfactant interactions, *J. Am. Oil Chem. Soc.*, **54**, 561–566 (1977).
- (5) C. U. Patel, Anti-static properties of some cationic polymers used in hair care products, *Int. J. Cosmet. Sci.*, **5**, 181–188 (1983).
- (6) Y. Suzuki and K. Yahagi, Dynamic and qualitative evaluation of combing force on human hair, *J. Soc. Chem. Jpn.*, **27**, 11–19 (1993).
- (7) Y. Hukuchi and U. Tamura, Instrumental methods for evaluating perceptible effects of shampoo and rinse on human hair, *Fragrance J.*, **17**, 30–38 (1989).
- (8) N. Ohyama, S. Kobayashi, Y. Kakizawa, and M. Miyuki, Effects of physical properties of anionic surfactant-cationic polymer complexes on the feel of rinsing shampoo, *S.C.C.J. 43rd Symp., Japan, 1998*, p. 31.
- (9) K. Hayakawa and J. C. T. Kwak, Surfactant-polyelectrolyte interactions. 1. Binding of dodecyltrimethylammonium ions by sodium dextran sulfate and sodium poly(styrenesulfonate) in aqueous solution in the presence of sodium chloride, *J. Phys. Chem.*, **86**, 3866–3870 (1982).
- (10) K. Ohbu, O. Hiraishi, and I. Kashiwa, Effect of quaternary substitution of hydroxyethylcellulose on binding of dodecyl sulfate, *J. Am. Oil Chem. Soc.*, **59**, 108–112 (1982).
- (11) K. Shirahama and M. Tashiro, Binding of 1-decylpyridinium bromide to poly(vinyl sulfate), *Bull. Chem. Soc. Jpn.*, **57**, 377 (1984).
- (12) J. Liu, N. Takizawa, K. Shirahama, H. Abe, and K. Sakamoto, Effect of polymer size on the polyelectrolyte-surfactant interaction, *J. Phys. Chem. B.*, **101**, 7520–7523 (1997).
- (13) P. Hansson and M. Almgren, Interaction of CnTAB with sodium (caboxymethyl)cellulose: Effect of polyion linear charge density on binding isotherms and surfactant aggregation number, *J. Phys. Chem.*, **100**, 9038–9046 (1996).
- (14) P. L. Dibin, C. H. Chew, and L. M. Gan, Complex formation between anionic polyelectrolytes and cationic/nonionic mixed micelles, *J. Colloid. Interface Sci.*, **128**(2), 566–576 (1989).
- (15) C. Wang and K. C. Tam, New insights on the interaction mechanism within oppositely charged polymer/surfactant systems, *Langmuir*, **18**, 6484–6490 (2002).
- (16) C. Wang and K. C. Tam, Interaction between polyelectrolyte and oppositely charged surfactant: Effect of charge density, *J. Phys. Chem. B.*, **108**, 8976–8982 (2004).
- (17) M. S. Vethamuthu, P. L. Dubin, M. Almgren, and Y. Li, Cryo-TEM of polyelectrolyte-micelle complexes, *J. Colloid. Interface Sci.*, **186**, 414–419 (1997).
- (18) F. Yeh, E. L. Sokolvo, A. R. Khokhlov, and B. Chu, Nanoscale supramolecular structures in the gels of poly(diallyldimethylammonium chloride) interacting with sodium dodecyl sulfate, *J. Am. Chem. Soc.*, **118**, 6615–6618 (1996).
- (19) M. Miyake and Y. Kakizawa, Study on the interaction between polyelectrolytes and oppositely charged ionic surfactants. Solubilized state of the complexes in the postprecipitation region, *Colloid Polymer. Sci.*, **280**, 18–23 (2002).
- (20) E. P. Geiduschek and A. Holtzer, Application of light scattering to biological systems: Deoxyribonucleic acid and the muscle proteins, *Adv. Biol. Med. Phys.*, **6**, 431–551 (1958).
- (21) P. S. Leung and E. D. Goddard, Gels from dilute polymer/surfactant solutions, *Langmuir*, **7**, 608–609 (1991).
- (22) E. D. Goddard, P. S. Leung, and K. A. P. Padmanabhan, Novel gelling structures based on polymer/surfactant systems, *J. Soc. Cosmet. Chem.*, **42**, 19–34 (1991).
- (23) M. Huldén, Hydrophobically modified urethane-ethoxylate (HEUR) associative thickeners. 1. Rheology of aqueous solutions and interactions with surfactants, *Colloids Surf. A*, **82**, 263–277 (1994).

